physical sciences forum

Proceeding Paper

Analysis of T2K and MINERνA Semi-Inclusive ν_μ–^{12}C Measurements

J. M. Franco-Patino, R. González-Jiménez, S. Dolan, M. B. Barbaro, J. A. Caballero, G. D. Megias and J. M. Udias

MDPI

https://doi.org/10.3390/psf2023008043

physical sciences forum

MDPI

Proceeding Paper

Analysis of T2K and MINERνA Semi-Inclusive $\nu_\mu - {}^{12}$C Measurements †

J. M. Franco-Patino [1,2,3,*], R. González-Jiménez [4], S. Dolan [5], M. B. Barbaro [2,3], J. A. Caballero [1,6], G. D. Megias [1,7] and J. M. Udias [4]

1 Departamento de Física Atómica, Molecular y Nuclear, Universidad de Sevilla, 41080 Sevilla, Spain
2 Dipartimento di Fisica, Università di Torino, Via P. Giuria 1, 10125 Torino, Italy
3 Istituto Nazionale di Fisica Nucleare (INFN), Sezione di Torino, 10125 Torino, Italy
4 Grupo de Física Nuclear, Departamento de Estructura de la Materia, Física Térmica y Electrónica and IPARCOS, Facultad de Ciencias Físicas, Universidad Complutense de Madrid, CEI Moncloa, 28040 Madrid, Spain
5 European Organization for Nuclear Research (CERN), 1211 Geneva, Switzerland
6 Instituto de Física Teórica y Computacional Carlos I, 18071 Granada, Spain
7 Research Center for Cosmic Neutrinos, Institute for Cosmic Ray Research, University of Tokyo, Kashiwa, Chiba 277-8582, Japan
* Correspondence: jfpatino@us.es
† Presented at the 23rd International Workshop on Neutrinos from Accelerators, Salt Lake City, UT, USA, 30–31 July 2022.

Abstract: We compare the semi-inclusive $\nu_\mu - {}^{12}$C cross-section measurements via T2K and MINERνA collaborations with the predictions from the SuSAv2-MEC model implemented in the neutrino event generator GENIE and an unfactorized approach based on the relativistic distorted wave impulse approximation (RDWIA). Results, which include cross-sections as a function of the final muon and proton kinematics as well as correlations between both, show that the agreement with data obtained via the RDWIA approach—which accounts for final-state interactions—matches or improves GENIE-SuSAv2 predictions for very forward angles, where scaling violations are relevant.

Keywords: neutrino physics; semi-inclusive neutrino–nucleus reactions; FSI modeling

Citation: Franco-Patino, J.M.; González-Jiménez, R.; Dolan, S.; Barbaro, M.B.; Caballero, J.A.; Megias, G.D.; Udias, J.M. Analysis of T2K and MINERνA Semi-Inclusive $\nu_\mu - {}^{12}$C Measurements. *Phys. Sci. Forum* **2023**, *8*, 43. https://doi.org/10.3390/psf2023008043

Academic Editor: Yue Zhao

Published: 22 August 2023

1. Introduction

Lately, there has been a growing interest in the measurements of more exclusive neutrino–nucleus reactions, for instance, the detection in the coincidence of a muon and an ejected proton in the final state, which are more sensitive to nuclear medium effects than inclusive measurements, where only the final lepton is detected. Such reactions, where both a lepton and another particle are detected in coincidence, are often referred as semi-inclusive reactions. Because an extra particle is detected alongside the lepton, these reactions do not fall under the category of inclusive, nor can they be classified as exclusive. This is due to the unknown energy transfer to the nucleus by the neutrino, leading to uncertainty about the state of the residual nucleus. In the past, an unfactorized relativistic and fully quantum approach based on the relativistic distorted-wave impulse approximation (RDWIA) [1] successfully described exclusive $(e, e'p)$ cross-section measurements using a relativistic optical potential (ROP) to model the final state interactions (FSIs) between the ejected proton and the residual nucleus. In contrast with the microscopic and unfactorized models like RDWIA, which incorporate in the modeling both the lepton–boson and the boson–nucleus vertex in some detail, and thus can be compared to semi-inclusive observables, there are other models, like the SuSAv2 model [2,3], that are aimed to describe inclusive cross-sections, that is, only as function of the final lepton kinematics, and thus cannot make predictions on both leptons and hadrons in the final state. In spite of this, by taking advantage of a factorization approach, some neutrino event generators like GENIE [4]

can make predictions about the lepton and also the outgoing nucleon kinematics from these inclusive models [5]. This factorization implies that the initial nuclear state, which is generated from a local Fermi gas distribution, is decoupled from the leptonic vertex. This way, while the behavior of the cross-section against the muon kinematics may be described correctly, there is no guarantee whatsoever that the correlations between the final muons and protons for a given event are preserved. Moreover, this approach could present inconsistent results when the nuclear model used to generate the outgoing nucleon is different from the nuclear model used in the inclusive cross-section, as is the case in the current SuSAv2 implementation in GENIE [5]. Furthermore, the results from this approach rely strongly on the semi-classical description of FSIs commonly used in neutrino event generators [6,7], which have been shown to be unable to produce microscopic FSI predictions at low outgoing nucleon momenta [8].

In this manuscript, we will compare T2K [9] and MINERνA [10,11] $\nu_\mu - ^{12}$C semi-inclusive CC0π cross-section measurements with one muon and at least one proton in the final state (denoted CC0πNp) with results obtained from the RDWIA using a ROP fitted to elastic proton–nucleus scattering data and a modified version of the relativistic mean field (RMF) potential [12,13] parameterized to reproduce properties of nuclei. To this comparison, we will also add the calculation without FSIs, using the relativistic plane-wave impulse approximation (RPWIA), to show the importance of this nuclear effect for the description of semi-inclusive results, and the estimations from the inclusive SuSAv2-MEC model implemented in the GENIE event generator [5] to test the validity of the approximations made by the event generators to obtain hadron kinematics, using as the starting point such an inclusive model. To all these quasielastic contributions, we will add the SuSAv2-2p2h meson exchange current (MEC) [14–16] and pion absorption contributions calculated with GENIE for a full comparison with the available cross-section measurements.

2. Semi-Inclusive Neutrino–Nucleus Reactions within the RDWIA

The kinematics of the outgoing lepton $\mathbf{k}'$ and nucleon $\mathbf{p_N}$ for semi-inclusive CC0π events is characterized by a set of six independent variables $(k', \theta_l, \phi_l, p_N, \theta_N^L, \phi_N^L)$ defined in the laboratory frame with the target nucleus A at rest and the neutrino direction fixed in the z-axis. We consider that the incoming neutrinos are distributed according to an energy distribution or flux $\Phi(k)$ and that the impulse approximation (IA) is valid. Then, the flux-averaged semi-inclusive neutrino–nucleus cross-section is [8,13]

$$\left\langle \frac{d\sigma}{dk' d\Omega_{k'} dp_N d\Omega_N^L} \right\rangle = \frac{G_F^2 \cos^2\theta_c k'^2 p_N^2}{64\pi^5} \int dk \frac{W_B}{E_B f_{\text{rec}}} L_{\mu\nu} H^{\mu\nu} \Phi(k), \tag{1}$$

where $\Omega_{k'}$ and Ω_N^L are, respectively, the solid angles of the final lepton and the ejected proton; the residual nucleus B can be left in an excited state with invariant mass W_B and total energy E_B; $L_{\mu\nu}$ and $H^{\mu\nu}$ are the leptonic and hadronic tensors; and f_{rec} is the recoil factor. Taking into account that we will describe the initial nuclear state as a product of RMF single-particle states labeled with a quantum number κ, we introduce the hadron tensor for each shell κ, given by

$$H_\kappa^{\mu\nu} = \rho_\kappa(E_m) \sum_{m_j, s_N} J^\mu_{\kappa, m_j, s_N} J^{\nu *}_{\kappa, m_j, s_N} \tag{2}$$

where $\rho_\kappa(E_m)$ is the missing energy density and J^μ_{κ, m_j, s_N} is the hadronic current that depends on the initial and final nucleons wave functions Ψ^{s_N} and $\Phi_\kappa^{m_j}$, and the one-body current operator [17]. The parameterization of missing energy density $\rho_\kappa(E_m)$ for ^{12}C used in this work is equivalent to the one used in [13] for ^{16}O. By using this method, we can include effects caused by long- and short-range correlations as seen in the spectral function formalism but without imposing factorization of the cross-section. The parameters in the $\rho_\kappa(E_m)$ function for ^{12}C were fitted to reproduce the missing energy profile that one

obtains from the Rome spectral function for ^{12}C [18,19]. The different FSI prescriptions are associated to the different ways of calculating $\Psi^{s_N}(\mathbf{p_N}, \mathbf{r})$, all of them within a fully relativistic and quantum framework.

Energy-dependent RMF (ED-RMF): For this model, the nucleon ejected in the final state is represented by a scattering solution of the Dirac equation with the same RMF potential used to describe the initial nucleus but multiplied by a phenomenological function that weakens the potential for increasing nucleon momenta [12].

Relativistic Optical Potential (ROP): The ejected nucleon moves across the residual hadronic system under the influence of a phenomenological relativistic optical potential fitted to reproduce elastic proton–nucleus scattering data [20] in the context of the optical model. This potential contains a real and an imaginary term, where the latter accounts for loses to inelastic channels.

Relativistic Plane-Wave IA (RPWIA): The ejected nucleon is described by a relativistic plane wave. Therefore, in this case, FSIs are neglected. We include this model in our study to assess the importance of FSIs in the description of semi-inclusive processes.

3. Results

We now proceed to compare all the available semi-inclusive CC0πNp cross-section measurements for T2K and MINERνA with the predictions of two approaches for the 1p1h sector: the RMF model based on Equation (1), where FSIs are implemented using the different prescriptions described in Section 2, and the 1p1h GENIE-SuSAv2 implementation described in [5]. For both approaches, we add on top of the SuSAv2-2p2h MEC [14,21] and pion absorption [22] contributions calculated with GENIE. The processing of the GENIE output and its comparison to experimental data was made using the NUISANCE framework [23]. For both T2K and MINERνA, the comparison is made as function of muon and proton kinematics, as well as a function of the transverse kinematic imbalances (TKI) [24] that measure correlations between the final muon and proton in the plane transverse to the neutrino direction.

In Figure 1, the semi-inclusive cross-sections predicted by ROP as a function of the muon and proton kinematics for MINERνA seem qualitatively in reasonable agreement with the theoretical predictions, except for the θ_N^L cross-section, where there is an underestimation of the cross-section measurements for low values of θ_N^L and an overestimation in the high-θ_N^L region. Whilst all models other than ROP overpredict the cross-section, agreement between the ED-RMF and the GENIE-SuSAv2 predictions is very good except for the p_N distribution, where differences can be seen in the whole interval of the proton momentum. It should be noted that the apparent overprediction of the non-ROP models may be due to a mismodeling of the strength of the 2p2h or pion absorption contributions and may therefore not suggest an issue in the CCQE modeling.

In Figure 1, we also compare the microscopic calculations and the GENIE implementation of SuSAv2 with T2K CC0π cross-section measurements without protons in the final state with momenta above 0.5 GeV (CC0π0p) as a function of the final muon kinematics (top-right panels) and the semi-inclusive CC0πNp cross-section measurements with protons in the final state with momenta above 0.5 GeV as a function of the final proton kinematics (bottom-right panels). For the CC0π0p results and backward muon angles, the microscopic calculation predicts a rather small difference between the results for RPWIA and the models with FSIs (ROP and ED-RMF), all of them underestimating the experimental measurements in contrast with the better agreement achieved with GENIE- SuSAv2. As we move to more forward angles, GENIE-SuSAv2 predictions start to overestimate some of the experimental points, an outcome probably due to the scaling/factorization violations and poor treatment of low-energy effects, which are accounted for more consistently in ED-RMF. The CC0πNp results shown in Figure 1 are more affected by non-quasielastic contributions than the CC0π0p measurements and the GENIE-SuSAv2 results slightly overestimate some of the experimental points, while the ED-RMF and ROP models tend to match or improve the agreement with the measurements.

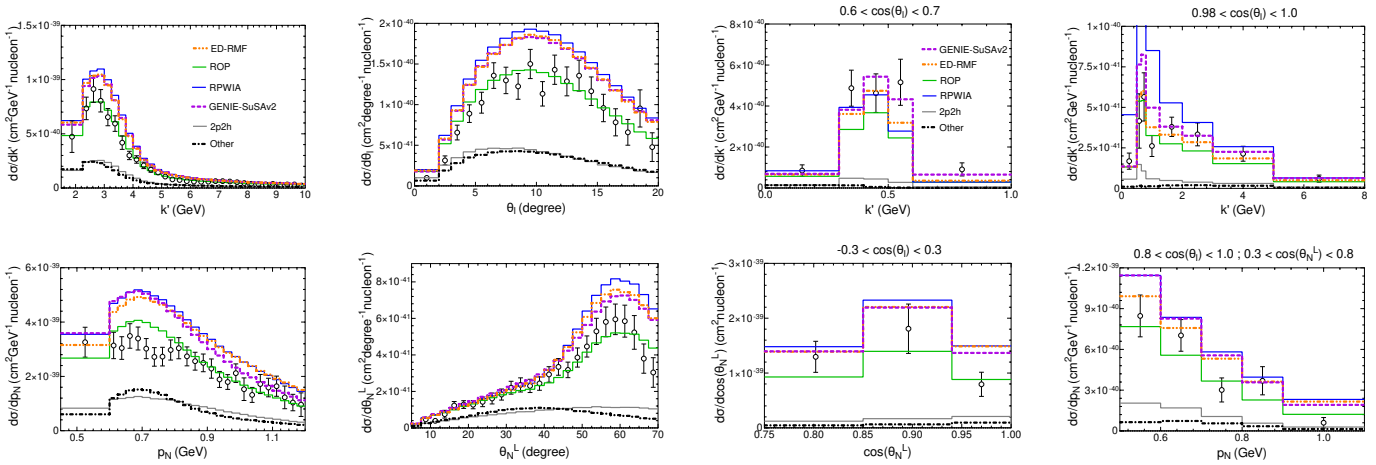

Figure 1. MINER νA [10,11] (**left**) and T2K [9] (**right**) CC0π semi-inclusive $\nu_\mu - ^{12}$C cross sections as a function of the muon (**top**) and proton (**bottom**) kinematics. All curves include the 2p2h and pion absorption contributions (also shown separately), evaluated using GENIE. T2K results as a function of the muon kinematics correspond to $p_N < 0.5$ GeV, while the results as a function of the proton kinematics correspond to $p_N > 0.5$ GeV.

Finally, in Figure 2, we show the predictions of the different models as a function of TKI compared with T2K and MINERνA measurements. The δp_T distribution favors the ED-RMF calculation over the GENIE-SuSAv2 predictions in the low δp_T region for T2K, which is mainly dominated by initial-state effects with negligible contribution from the 2p2h and pion absorption channels. This could be caused by the inconsistencies of the implementation of the SuSAv2 model, which is based on the RMF theory, in GENIE, that generates the initial state nucleon using a local Fermi gas model. Above the Fermi level, all the microscopic models except for ROP overestimate T2K δp_T measurements after including the 2p2h and pion absorption contributions. Regarding the MINERνA δp_T measurements, all the models except for ROP overestimate the data in the peak of the distribution even without adding the non-quasielastic contributions. In the high-momentum imbalance tail, the contribution from non-quasielastic channels is sufficient and necessary to match the experimental results. Concerning the $\delta\alpha_T$ distributions, it is interesting to point out the appearance of a clear peak at large $\delta\alpha_T$ values in the MINERνA cross-section measurements that is not present in the T2K experimental results, which might be caused by additional non-quasielastic contributions present in MINERνA but not in T2K due to the higher energy of the neutrinos. The GENIE-SuSAv2 predictions and all the microscopic results except for the ROP overestimate the cross-section measurements, although the shape of the rise in $\delta\alpha_T$ for MINERνA seems to be well described by the combination of FSIs and non-quasielastic contributions and the overestimation is less significant using ED-RMF compared with GENIE-SuSAv2 results. Lastly, all the model predictions except for ROP as a function of $\delta\phi_T$ shown in Figure 2 overestimate the cross-section measurements, although the overestimation is less severe in the case of the ED-RMF model for low values of $\delta\phi_T$.

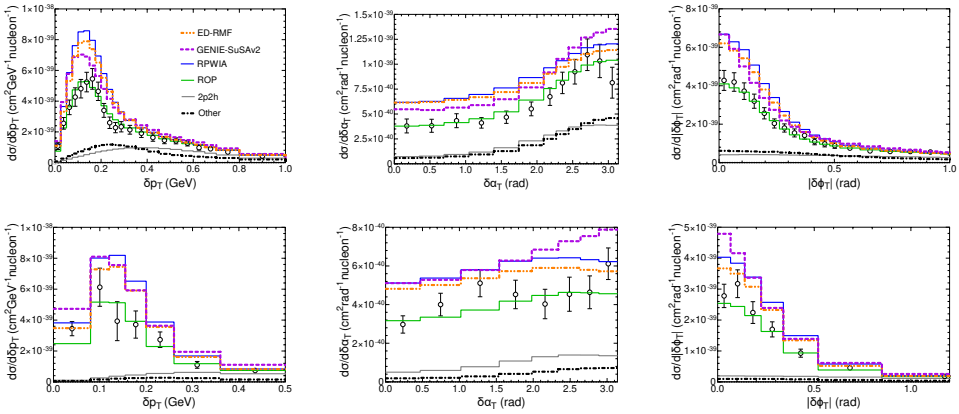

Figure 2. MINER νA [10,11] (**top**) and T2K [9] (**bottom**) CC0π semi-inclusive $\nu_\mu - {}^{12}$C cross-sections as a function of the transverse kinematic imbalances δp_T, $\delta\alpha_T$ and $|\delta\phi_T|$. All curves include the 2p2h and pion absorption contributions (also shown separately), evaluated using GENIE.

4. Conclusions

We have compared the treatment of semi-inclusive neutrino–nucleus reactions within an unfactorized relativistic approach with the GENIE implementation of the SuSAv2-MEC model and some of the latest T2K and MINERνA cross-section measurements. Although it is difficult to draw precise conclusions about the individual effects of the approximations used to obtain semi-inclusive results with the SuSAv2 model, the microscopic calculation using a modified RMF potential (ED-RMF) improves the agreement with the experimental results at forward angles where scaling violations and low-energy effects not included in the SuSAv2 model are relevant. For the cross-sections as a function of the TKI, the best agreement with the experimental data is given by the RDWIA predictions, especially the MINERνA measurements, where ROP is the only model that does not overestimate the data.

Author Contributions: Writing—original draft preparation, J.M.F.-P.; writing—review and editing, R.G.-J., S.D., M.B.B., J.A.C., G.D.M. and J.M.U.; visualization, J.M.F.-P. All authors have read and agreed to the published version of the manuscript.

Funding: This research was funded by the projects PID2020-114687GB-100; PID2021-127098NA-I00 funded by MCIN/AEI/10.13039/501100011033/FEDER, UE; PR65/19-22430 funded by the government of Madrid and Complutense University; FQM160, SOMM17/61015/UGR and P20-01247 funded by Junta de Andalucía. It is supported in part by the University of Tokyo ICRR's Inter-University Resarch Program FY2021 & FY2022; by the European Union's Horizon 2020 research and innovation programme under the Marie Sklodowska-Curie grant agreement No. 839481; by the University of Turin, project BARM-RILO-21; and by INFN, national project NUCSYS. J.M. Franco-Patino acknowledges support from a fellowship from the Ministerio de Ciencia, Innovación y Universidades, Program FPI (Spain).

Institutional Review Board Statement: Not applicable.

Informed Consent Statement: Not applicable.

Data Availability Statement: Not applicable.

Conflicts of Interest: The authors declare no conflict of interest.

References

1. Udías, J.M.; Caballero, J.A.; de Guerra, E.M.; Vignote, J.R.; Escuderos, A. Relativistic mean field approximation to the analysis of ${}^{16}\mathrm{O}(e,e'p){}^{15}\mathrm{N}$ data at $|Q^2| > ;\ 0.4(\mathrm{GeV}/c)^2$. *Phys. Rev. C* **2001**, *64*, 024614. [CrossRef]
2. González-Jiménez, R.; Megias, G.D.; Barbaro, M.B.; Caballero, J.A.; Donnelly, T.W. Extensions of superscaling from relativistic mean field theory: The SuSAv2 model. *Phys. Rev. C* **2014**, *90*, 035501. [CrossRef]

3. Megias, G.D.; Barbaro, M.B.; Caballero, J.A.; Donnelly, T.W. Inclusive electron scattering within the SuSAv2 meson-exchange current approach. *Phys. Rev. D* **2016**, *94*, 013012. [CrossRef]
4. Andreopoulos, C.; Barry, C.; Dytman, S.; Gallagher, H.; Golan, T.; Hatcher, R.; Perdue, G.; Yarba, J. The GENIE Neutrino Monte Carlo Generator: Physics and User Manual. *arXiv* **2015**, arXiv:1510.05494.
5. Dolan, S.; Megias, D.; Bolognesi, S. Implementation of the SuSAv2-meson exchange current 1p1h and 2p2h models in GENIE and analysis of nuclear effects in T2K measurements. *Phys. Rev. D* **2020**, *101*, 033003. [CrossRef]
6. Dytman, S.A.; Meyer, A.S. Final State Interactions in GENIE. *AIP Conf. Proc.* **2011**, *1405*, 213–218.
7. Golan, T.; Juszczak, C.; Sobczyk, J.T. Effects of final-state interactions in neutrino-nucleus interactions. *Phys. Rev. C* **2012**, *86*, 015505. [CrossRef]
8. Nikolakopoulos, A.; González-Jiménez, R.; Jachowicz, N.; Niewczas, K.; Sánchez, F.; Udías, J.M. Benchmarking intra-nuclear cascade models for neutrino scattering with relativistic optical potentials. *arXiv* **2022**, arXiv:2202.01689.
9. Abe, K.; Amey, J.; Andreopoulos, C.; Anthony, L.; Antonova, M.; Aoki, S.; Ariga, A.; Ashida, Y.; Azuma, Y.; Ban, C.; et al. Characterization of nuclear effects in muon-neutrino scattering on hydrocarbon with a measurement of final-state kinematics and correlations in charged-current pionless interactions at T2K. *Phys. Rev. D* **2018**, *98*, 032003. [CrossRef]
10. Lu, X.G.; Betancourt, M.; Walton, T.; Akbar, F.; Aliaga, L.; Altinok, O.; Andrade, D.A.; Ascencio, M.; Bellantoni, L.; Bercellie, A.; et al. Measurement of Final-State Correlations in Neutrino Muon-Proton Mesonless Production on Hydrocarbon at $<E_\nu> = 3$ GeV. *Phys. Rev. Lett.* **2018**, *121*, 022504. [CrossRef]
11. Cai, T.; Lu, X.-G.; Harewood, L.A.; Wret, C.; Akbar, F.; Andrade, D.A.; Ascencio, M.V.; Bellantoni, L.; Bercellie, A.; Betancourt, M.; et al. Nucleon binding energy and transverse momentum imbalance in neutrino-nucleus reactions. *Phys. Rev. D* **2020**, *101*, 092001. [CrossRef]
12. González-Jiménez, R.; Barbaro, M.B.; Caballero, J.A.; Donnelly, T.W.; Jachowicz, N.; Megias, G.D.; Niewczas, K.; Nikolakopoulos, A.; Udías, J.M. Constraints in modeling the quasielastic response in inclusive lepton-nucleus scattering. *Phys. Rev. C* **2020**, *101*, 015503. [CrossRef]
13. González-Jiménez, R.; Barbaro, M.B.; Caballero, J.A.; Donnelly, T.W.; Jachowicz, N.; Megias, G.D.; Niewczas, K.; Nikolakopoulos, A.; Van Orden, J.W.; Udías, J.M. Neutrino energy reconstruction from semi-inclusive samples. *Phys. Rev. C* **2022**, *105*, 025502. [CrossRef]
14. Simo, I.R.; Amaro, J.E.; Barbaro, M.B.; De Pace, A.; Caballero, J.A.; Megias, G.D.; Donnelly, T.W. Emission of neutron–proton and proton–proton pairs in neutrino scattering. *Phys. Lett. B* **2016**, *762*, 124–130. [CrossRef]
15. Megias, D.; Donnelly, W.; Moreno, O.; Williamson, F.; Caballero, A.; González-Jiménez, R.; De Pace, A.; Barbaro, B.; Alberico, M.; Nardi, M.; et al. Meson-exchange currents and quasielastic predictions for charged-current neutrino-^{12}C scattering in the superscaling approach. *Phys. Rev. D* **2015**, *91*, 073004. [CrossRef]
16. Megias, D.; Amaro, E.; Barbaro, B.; Caballero, A.; Donnelly, W.; Simo, I.R. Charged-current neutrino-nucleus reactions within the superscaling meson-exchange current approach. *Phys. Rev. D* **2016**, *94*, 093004. [CrossRef]
17. Franco-Patino, J.M.; Gonzalez-Rosa, J.; Caballero, J.A.; Barbaro, M.B. Semi-inclusive charged-current neutrino-nucleus cross sections in the relativistic plane-wave impulse approximation. *Phys. Rev. C* **2020**, *102*, 064626. [CrossRef]
18. Benhar, O.; Fabrocini, A.; Fantoni, S.; Sick, I. Spectral function of finite nuclei and scattering of GeV electrons. *Nuclear Phys. A* **1994**, *579*, 493–517. [CrossRef]
19. Benhar, O.; Farina, N.; Nakamura, H.; Sakuda, M.; Seki, R. Electron- and neutrino-nucleus scattering in the impulse approximation regime. *Phys. Rev. D* **2005**, *72*, 053005. [CrossRef]
20. Cooper, E.D.; Hama, S.; Clark, B.C. Global Dirac optical potential from helium to lead. *Phys. Rev. C* **2009**, *80*, 034605. [CrossRef]
21. Simo, I.R.; Amaro, J.E.; Barbaro, M.B.; De Pace, A.; Caballero, J.A.; Donnelly, T.W. Relativistic model of 2p-2h meson exchange currents in (anti)neutrino scattering. *J. Phys. G* **2017**, *44*, 065105. [CrossRef]
22. Berger, C.; Sehgal, L.M. Lepton mass effects in single pion production by neutrinos. *Phys. Rev. D* **2007**, *76*, 113004. [CrossRef]
23. Stowell, P.; Wret, C.; Wilkinson, C.; Pickering, L.; Cartwright, S.; Hayato, Y.; Mahn, K.; McFarland, K.S.; Sobczyk, J.; Terri, R. NUISANCE: A neutrino cross-section generator tuning and comparison framework. *J. Instrum.* **2017**, *12*, P01016. [CrossRef]
24. Lu, X.-G.; Pickering, L.; Dolan, S.; Barr, G.; Coplowe, D.; Uchida, Y.; Wark, D.; Wascko, M.O.; Weber, A.; Yuan, T. Measurement of nuclear effects in neutrino interactions with minimal dependence on neutrino energy. *Phys. Rev. C* **2016**, *94*, 015503. [CrossRef]